Isomerization and intermolecular solute–solvent interactions of ethyl isocyanate: Ultrafast infrared vibrational echoes and linear vibrational spectroscopy

Nancy E. Levinger,[a] Paul H. Davis,[b] Pradipta Kumar Behera,[c] D. J. Myers,[d] Christopher Stromberg, and M. D. Fayer[e]
Department of Chemistry, Stanford University, Stanford, California 94305

(Received 19 August 2002; accepted 17 October 2002)

Thermally induced *gauche–trans* isomerization and direct solute–solvent interactions of the solute, ethyl isocyanate (EIC), in the solvent, 2-methylpentane (2MP), are investigated using ultrafast infrared vibrational echo experiments and linear vibrational absorption spectroscopy of the isocyanate (N=C=O) antisymmetric stretching mode (2278 cm^{-1}). Both the EIC vibrational echo measured pure vibrational dephasing and the absorption spectra show complex behavior as a function of temperature from room temperature to 8 K. The EIC data are compared to absorption experiments on the same mode of isocyanic acid (HNCO), which cannot undergo isomerization. To describe the observations, a model is presented that involves both intramolecular dynamics and intermolecular dynamical interactions. At room temperature, *gauche–trans* isomerization is very fast, and the isomerization dynamics contribution to the vibrational echo decay and the absorption line shape is small because it is motionally narrowed. The dominant contribution to both the vibrational echo decay and the absorption spectrum is from direct dynamical interactions of the solute with the solvent. As the temperature is lowered, the direct contribution to vibrational dephasing decreases rapidly, but the contribution from isomerization increases because the extent of motional narrowing diminishes. The combined effect is a very gradual decrease of the rate of pure dephasing as the temperature is initially lowered from room temperature. At very low temperature, below the 2MP glass transition, isomerization cannot occur. The absorption spectrum displays two peaks, interpreted as the distinct *gauche* and *trans* absorption bands. Even at 8 K, the pure dephasing is surprisingly fast. The direct solvent-induced dephasing is negligible. The dephasing is caused by motions of the ethyl group without isomerization occuring. At intermediate temperatures ($150\,K > T > 100\,K$), isomerization takes place, but its contribution to the pure dephasing is not motionally narrowed. The absorption spectral shapes are complex. Dephasing arising from direct interaction with the solvent is small. Both isomerization and fluctuations on the *gauche–trans* surface contribute to the absorption line shape. The model that is used to describe the results involves a NMR type exchange calculation with additional contributions from the direct solvent interactions that are obtained from the temperature-dependent HNCO IR spectra. From the temperature dependence of the isomerization ''jump'' rate, the barrier height for the isomerization is found to be $\sim 400\ cm^{-1}$. © *2003 American Institute of Physics.* [DOI: 10.1063/1.1527926]

I. INTRODUCTION

A vibrational absorption spectrum of a solute mode in a solvent reflects all of the dynamics of processes that are coupled to the mode. The line shape and linewidth of the spectrum are sensitive to both intramolecular and intermolecular interactions. However, it is difficult to separate the various influences on a mode through an absorption spectrum alone. Processes on all time scales affect the spectrum. For example, in a glassy solvent, the variety of essentially static local solvent environments will give rise to inhomogeneous broadening of the spectrum.[1] Dynamics that may occur can be totally masked by inhomogeneous broadening. Even in a liquid at room temperature, a variety of processes, such as the vibrational lifetime and pure dephasing, can contribute to line broadening.[2]

In this paper, dynamics of ethyl isocyanate (EIC) in the solvent, 2-methylpentane (2MP), are investigated by examining the temperature dependences of the isocyanate (N=C=O) antisymmetric stretching mode's absorption spectrum (centered near 2280 cm^{-1}) and ultrafast infrared vibrational echo decay. By combining the spectral data and the vibrational echo data, an interesting, but complex, picture of the EIC dynamics emerges. The ethyl group can sample a range of conformations. Electronic structure calculations of the isolated molecule[3] show that *trans* and *gauche* forms

[a]Permanent address: Department of Chemistry, Colorado State University, Fort Collins, Colorado 80523.
[b]Current address: Department of Chemistry & Biochemistry, University of California at San Diego, La Jolla, California 92093-0303.
[c]Permanent address: Department of Chemistry, Sambalpur University, Jyoti Vihar, Sambalpur, PIN—768019, India.
[d]Permanent address: Alexza Molecular Delivery Corporation, Palo Alto, California 94303.
[e]Corresponding author. Electronic mail: fayer@stanford.edu

 © 2003 American Institute of Physics

should be stable, while the *cis* conformation is a saddle point on the potential surface. While the calculated potential surface must be considered an approximation for the molecule in a liquid, it shows that the *trans* configuration is only somewhat higher in energy than the *gauche*, and the barrier is relatively low. The two conformations are also calculated to give somewhat different vibrational frequencies for the isocyanate antisymmetric stretch.[3,4]

Because of the low barrier and small energy difference between the isomers, rapid switching of conformations would be expected at room temperature. For fast enough exchange, the two vibrational transitions associated with the *trans* and *gauche* conformations will be motionally narrowed into a single line.[5–7] In fact, at room temperature a single line is observed, while at low temperature the line separates into two overlapping peaks. Comparisons to the spectrum of isocyanic acid, H–N=C=O (HNCO), which cannot undergo *trans–gauche* isomerization, and detailed vibrational echo experiments show that there are several contributions to the line shape that vary in importance with temperature. The line shape and the vibrational pure dephasing time, T_2^*, are influenced by intermolecular and intramolecular processes. The intermolecular processes involve the direct interaction of the isocyanate asymmetric stretch with solvent dynamics. The intramolecular dynamics are isomerization at high temperatures and motions on the isomerization potential surface that do not result in isomerization at low temperatures.

At high temperature, the solvent dynamics are the dominant contribution to the spectrum and the pure dephasing. The major contribution of the intermolecular dynamics is demonstrated by the broad Lorentzian line width of HNCO, which lacks contributions from intramolecular ethyl dynamics. At room temperature, the HNCO linewidth is almost identical to that of EIC. As the temperature is lowered, the HNCO linewidth narrows very rapidly; in contrast, the EIC T_2^* measured with vibrational echoes and the EIC spectroscopic linewidth change very slowly. A model is presented that treats the isomerization in terms of a NMR-type exchange formalism combined with the other contributions to the line shape and the pure dephasing. The analysis using the model demonstrates that as the temperature is lowered, the direct contribution to vibrational dephasing decreases rapidly, but the contribution from isomerization increases because the extent of motional narrowing lessens. The tradeoff between the decreasing direct solvent contribution and the increasing isomerization contribution makes both the pure dephasing and the EIC line shape change relatively slowly with temperature down to ~120 K.

As the temperature is decreased, isomerization slows and then ceases. The single peak observed in the high-temperature absorption spectrum develops two distinct spectral features attributable to the *trans* and *gauche* configurations of EIC. Surprisingly, even at the lowest temperature probed, 8 K, the dephasing is still fast. At low temperatures, direct solvent-induced dephasing is negligible. Instead, the dephasing arises from fluctuations of the ethyl group without isomerization occuring. At intermediate temperatures ($150\,\mathrm{K} > T > 100\,\mathrm{K}$), the absorption spectral shapes are complex. Isomerization takes place, but its contribution to the pure dephasing is not motionally narrowed. A direct interaction with the solvent impacts the dephasing to some extent, and the dephasing and the absorption line shape have contributions from both isomerization and fluctuations on the *gauche–trans* surface.

The combination of experiments and the model calculations provide a very complete description of the processes under observation. The model calculations are quantitative, but because of assumptions used to untangle the data, there may be some systematic error in the analysis. Therefore, temperature-dependent isomerization jump times that emerge from the data fitting may have some error. Nonetheless, the experiments demonstrate that by using a combination of vibrational echo experiments and conventional vibrational spectroscopy it is possible to observe isomerization, a very basic chemical structural change on the electronic ground state potential surface that is induced thermally. Furthermore, the data analysis yields a estimate of the barrier for isomerization of $400 \pm 50\ \mathrm{cm}^{-1}$.

II. EXPERIMENTAL METHODS

A. Sample preparation

Ethyl isocyanate (EIC, Aldrich, 98% purity) was purchased from Aldrich and distilled prior to use. After distillation the EIC was stored at low temperature to minimize degradation of the molecule via hydrolysis. 2-methylpentane (2MP, Aldrich, 99+% purity) was used as received and stored over molecular sieves after opening to prevent the uptake of water. Samples were prepared in a low humidity environment to minimize hydrolysis.

Isocyanic acid (HNCO) was synthesized by a dropwise addition of a saturated aqueous solution of potassium cyanate (KOCN, Aldrich, 96% purity) to concentrated phosphoric acid (Baker, 85% by weight in water), according to the method of Ashby and Werner.[8] The resultant HNCO gas was passed through a trap cooled by a dry ice/acetone bath to remove volatiles before being bubbled through 2MP. FTIR spectra confirmed the presence of HNCO in 2MP solution. Unfortunately, because the N=C=O antisymmetric stretch of HNCO in 2MP occurs at the same wavelength as the antisymmetric stretch of CO_2, we were precluded from performing laser-based experiments on this molecule due to atmospheric absorption of the laser beam.

Custom optical cuvettes consisting of a copper body with CaF_2 windows secured by copper flanges were used for both the steady-state and time-resolved experiments. Variable thickness Teflon spacers placed between the CaF_2 windows determined the pathlength of the cells. For all experiments reported in this paper, the pathlength used was 400 μm. A 100 μm diameter stainless steel pinhole was also placed between the cuvette windows to assist in the spatial overlap of the laser beams in the sample. Initially, a decomposition product appeared in some of the EIC samples several days after injection into the copper sample cells. On the basis of the possible chemical reactions that the EIC can undergo[9] and the position of the peak in the IR spectrum corresponding to the decomposition product, we believe that the decomposition product was CO_2 dissolved in the 2MP.

To prevent this decomposition from occurring, sample cells were carefully cleaned and dried in an oven prior to use.

For measurements of steady-state spectra, a closed-cycle He refrigerator cooled the samples, while for the time-resolved studies the samples were cooled in a constant-flow cryostat using either liquid nitrogen or liquid helium. The temperature of the samples was monitored via a silicon diode temperature sensor (Lakeshore Cryotronics Model DT-470-SD-11; accuracy of better than ± 0.5 K, 100–305 K, better than ± 0.25 K, 2–100 K) mounted to the exterior of the cuvette window with thermally conducting low-temperature epoxy. Temperature regulation (temperature stability ± 0.02 K or better) was accomplished using a second silicon diode temperature sensor linked to a feedback temperature controller.

B. Spectroscopy

Steady-state IR spectra with 0.25 cm^{-1} resolution were collected using a FTIR (Mattson). All spectra reported represent an average of 64 individual scans.

The laser system used for the time-resolved studies has been described in detail previously.[10] Here we describe certain modifications of the basic system unique to these studies. Briefly, the output of a home-built mode-locked Ti:Sapphire oscillator was temporally stretched in a curved mirror/grating stretcher. The band width was limited to 25 cm^{-1} by introducing a slit into the stretcher. The light was then amplified in a regenerative amplifier and recompressed using a single grating compressor. The output pulse was ~1 mJ, centered at 800 nm, with a pulse duration of ~750 fs.

The amplified Ti:Sapphire pulses were then used to create tunable IR light in a multistage OPA. Because the pulses were relatively long, the white light continuum used to seed the OPA was generated in a 6 mm long Nd:YAG crystal.[11] The continuum seed was mixed in an 8 mm Type I BBO crystal with part of the 800 nm light from the regenerative amplifier to produce signal and idler beams at 1.35 and 1.95 μm, respectively. The idler beam was then bandwidth limited using a grating (600 grooves/mm) and used to seed a second BBO crystal (8 mm long, Type II). The amplified signal and idler were then difference mixed in a 2 mm long Type II $AgGaS_2$ crystal to produce tunable mid-IR light. For the experiments reported here, the resulting 5 μJ pulses were centered at 2278 cm^{-1} with a bandwidth (FWHM) of ~25 cm^{-1}.

The mid IR pulses were split into strong (90%) and weak (10%) beams that traversed different paths before crossing in the sample. The weak beam was chopped at 500 Hz and directed along a variable pathlength delay line. The probe beam polarization could be controlled by a ZnSe Brewster-plate polarizer in its path. A small amount of the mid-IR light was split off and used for shot-to-shot normalization. Signal and reference beams impinged on liquid nitrogen cooled MCT detectors whose outputs were processed by gated integrators, divided by an analog processor, and input to a lock-in amplifier. The output of the lock-in was read into a computer using an A/D board.

The IR pulse duration was measured by autocorrelation in a 1 mm-long Type I $AgGaS_2$ crystal. The ~750 fs pulses were very nearly Gaussian in shape. The spectrum of the pulses was also close to Gaussian. The pulses were always within a factor of 1.4 or less of the transform limit (i.e., 1.4 times the Gaussian time–bandwidth product of 0.44). Extensive tests for power dependence were performed, and the beams were attenuated to eliminate saturation, heating, and other power-dependent effects.

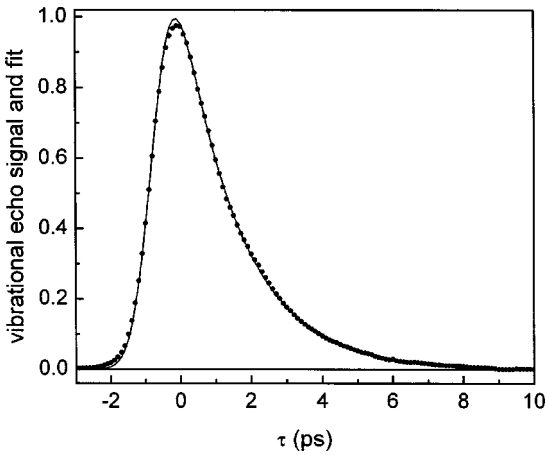

FIG. 1. Representative vibrational echo data of the N=C=O antisymmetric stretching mode of ethyl isocyanate in 2-methylpentane at 22 K. The solid line through the points is a fit to a single exponential decay convolved with a Gaussian instrument response function obtained from the autocorrelation of the infrared pulses.

III. RESULTS

A. Vibrational echo experiments

Figure 1 displays vibrational echo data (circles) taken on the antisymmetric N=C=O stretching mode of EIC in 2MP at 22 K. The solid line through the points is a fit to a single exponential decay convolved with a Gaussian instrument response function obtained from the autocorrelation of the infrared pulses. As discussed below, at this and other low temperatures, the vibrational echo decays are in the inhomogeneous limit, that is, the inhomogeneous linewidth is large compared to the dynamic linewidth.[12,13] Therefore, the dephasing time, T_2, can be obtained directly from the vibrational echo decay, and T_2 is four times the vibrational echo decay time, $T_2 = 4\tau_{\text{echo}}$.[12,13] At 22 K, $T_2 = 6.6$ ps, which corresponds to a dynamic linewidth $(1/\pi T_2)$ of 1.6 cm^{-1}.

Within experimental error, the vibrational echo decays are exponential at all temperatures, but they are not all in the inhomogeneous broadening limit. Figure 2(A) displays the vibrational echo decay times as a function of temperature. Figure 2(B) displays the vibrational lifetimes as a function of temperature measured with infrared pump–probe experiments. For an exponential decay of the vibrational echo signal characterized by the dynamic dephasing time, T_2, there are three contributions:

$$\frac{1}{T_2} = \frac{1}{T_2^*} + \frac{1}{2T_1} + \frac{1}{3T_{\text{or}}}. \tag{1}$$

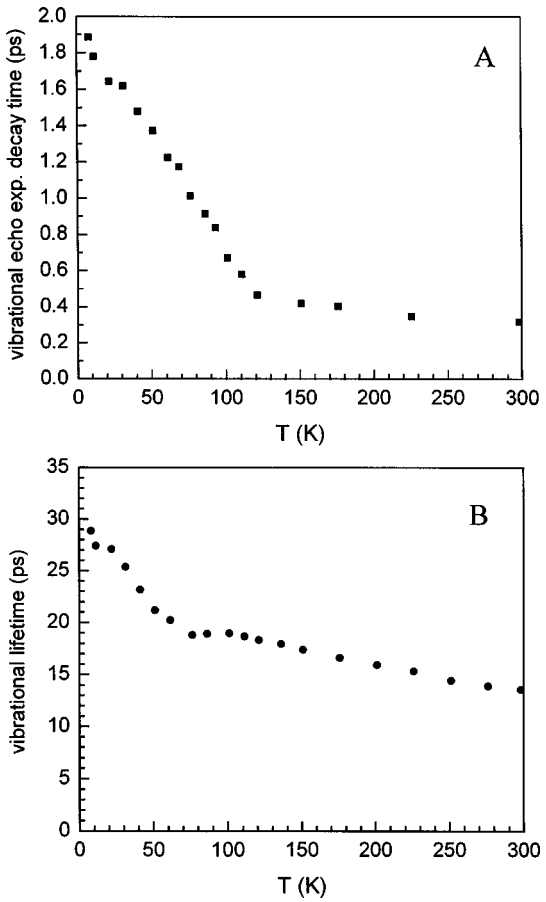

FIG. 2. (A) Vibrational echo decay time constants, T_2, and (B) vibrational lifetimes measured with infrared pump–probe experiments, T_1, of the N=C=O antisymmetric stretching mode of ethyl isocyanate in 2-methylpentane as a function of temperature.

T_2^* is the pure dephasing time; T_1 is the vibrational lifetime; and T_{or} is the orientational relaxation time. Using the Debye–Stokes–Einstein equation,[14] T_{or} was estimated to be ~7.5 ps at room temperature. This contribution to T_2 is negligible at room temperature, and because of the rapid increase in viscosity as the temperature is decreased, T_{or} makes a negligible contribution at all temperatures. Therefore, it is not considered further. $\frac{1}{2}T_1$ is very small compared to $1T_2$ at the highest temperatures, but it makes a small contribution at the lower temperatures (see Fig. 2). Therefore, Eq. (1) is used below to remove the lifetime contribution from the experimentally determined dephasing times to obtain the temperature-dependent pure dephasing times, T_2^*. T_2^* is related to the fluctuations in the vibrational transition energy, which is of interest here.

At the lowest temperatures, the inhomogeneous width is significantly greater than the dynamic linewidth, $1/\pi T_2$. Thus, the vibrational echo decay is in the inhomogeneous limit, and T_2 can be obtained directly from the vibrational echo decay time. At the highest temperature probed, the system is in the homogeneous limit. In this limit, T_2 is $2\tau_{\text{echo}}$.[12] This is confirmed by a comparison of the EIC antisymmetric stretching mode absorption spectrum linewidth with the dynamic linewidth, $1/\pi T_2$. The absorption line shape is Lorentzian at high temperatures, and the absorption width matches the vibrational echo-determined linewidth within experimental error.

Between the low-temperature (inhomogeneous line) and high-temperature (homogeneous line) limits, the system falls in an intermediate regime. The vibrational echo decay data at intermediate temperatures can be analyzed by fitting it to the appropriate decay function. In principle, eight double-sided Feynman diagrams contribute to the analysis of the data.[12] Three of these are rephasing diagrams that give rise to the vibrational echo decay after $\tau=0$. However, the laser bandwidth (25 cm^{-1}) is sufficient to span the 0–1 transition but is small compared to vibrational anharmonicity.[4] Therefore, the rephasing diagram that involves the 1–2 transition does not contribute to the vibrational echo decay. This is confirmed by the absence of anharmonic beats on the vibrational echo decay.[15–17] The other five diagrams contribute at negative times and only around $\tau=0$. They determine the shape of the rising edge of the signal. To simplify the calculations, the rising edge of the data is described in terms of an instrument response function, that is, the Gaussian pulse shape convolved with the square of the pulse shape. This reflects the fact that there is a single interaction of the radiation field with the system during the first pulse but two interactions with the second pulse. Then for exponential vibrational echo decays, the signal for a delta function pulse is[12]

$$S(\tau)=\int_0^\infty dt\,\exp[-\Delta^2(t-\tau)^2]\exp[-2(t+\tau)/T_2], \quad (2)$$

where Δ is the inhomogeneous linewidth in rad/s. Equation (2) is then convolved with the instrument response function.

As discussed in detail below, the absorption spectrum at very low temperatures consists of two lines: one corresponding to the *gauche* conformation of the ethyl group and one corresponding to the *trans* conformation. These can be approximated well as the sum of two overlapping Gaussian lines at the lowest temperatures. At high temperature, a rapid interchange of the conformations produces an absorption spectrum that is a single line. To account for the two transitions, Eq. (2) can be extended to give

$$\begin{aligned} S(\tau)=&a_1^2\int_0^\infty dt\,\exp[-\Delta_1^2(t-\tau)^2]\exp[-(t+\tau)/T_2] \\ &+a_2^2\int_0^\infty dt\,\exp[-\Delta_2^2(t-\tau)^2]\exp[-(t+\tau)/T_2] \\ &+a_1a_2\int_0^\infty dt\,2\cos(\omega(t-\tau)) \\ &\times\exp[-(\Delta_1^2+\Delta_2^2)(t-\tau)^2/2]\exp[-(t+\tau)/T_2], \quad (3) \end{aligned}$$

where Δ_1 and Δ_2 are the inhomogeneous widths of the individual lines and ω is the splitting between them. Amplitudes a_1 and a_2 are obtained from a fit of the steady-state spectrum to a sum of two Gaussians. Equation (3) is then convolved with the instrument response function.

Figure 3 displays fits to Eq. (3) for several datasets at intermediate temperatures, where the system is neither in the inhomogeneous nor homogeneous broadening limits. The quality of the fits is good. The pure dephasing times T_2^* are

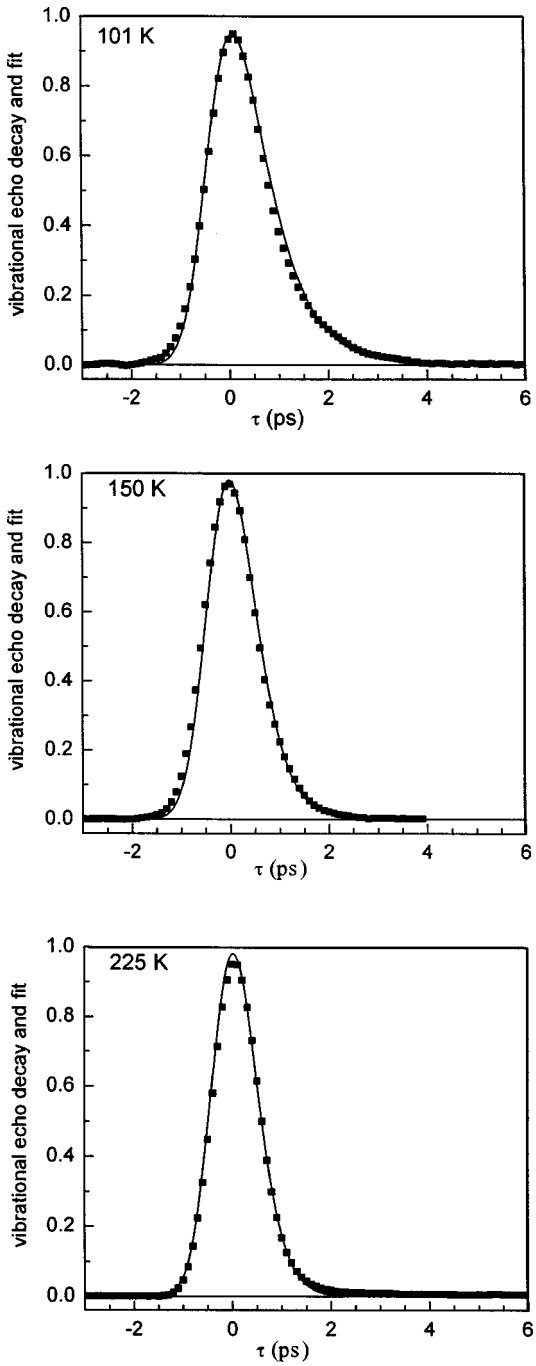

FIG. 3. Fits of vibrational echo decays at three temperatures to Eq. (3) convolved with a Gaussian instrument response function (see the text).

shown in Fig. 4. The data display a number of interesting features. First, from room temperature down to ~120 K, the change in the pure dephasing time with temperature is very mild. Then, at ~120 K, the temperature dependence appears to change slope rather suddenly. From 120 to 8 K, the lowest temperature studied, the increase in T_2^* with decreasing temperature is much steeper than at high temperature. Both the high temperature and low temperature portions of the data appear approximately linear, but with very different slopes. Also, at the lowest temperatures, T_2^* is relatively fast. In other vibrational echo experiments, the total dynamic dephasing (T_2) is dominated by the vibrational lifetime at

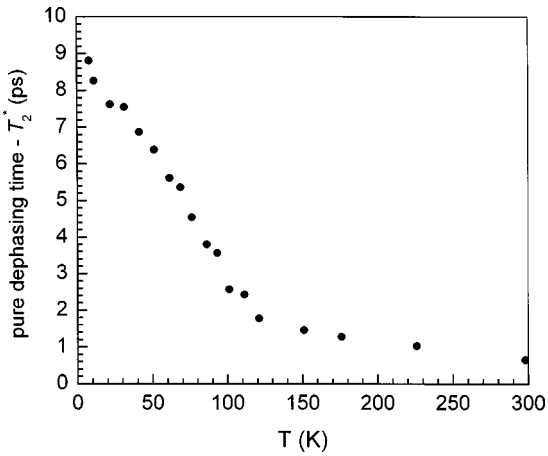

FIG. 4. Pure dephasing times, T_2^*, as a function of temperature for the N=C=O antisymmetric stretching mode of ethyl isocyanate in 2-methylpentane.

low temperature.[1] By 8 K, one might expect $T_2 = \sim 2T_1$. However, in this system, pure dephasing is the dominant contribution to the dynamic dephasing, even at 8 K, where the solvent is a glass far below T_g.

B. Linear absorption spectroscopy

An understanding of the temperature-dependent dynamics of EIC can be obtained by combining results from the vibrational echo experiments with temperature-dependent linear absorption measurements of the antisymmetric N=C=O stretch of both EIC and isocyanic acid (HNCO). Like the vibrational echoes, the linear spectroscopy of the EIC N=C=O antisymmetric stretching mode does not display a simple temperature dependence. Representative steady-state IR absorption spectra of EIC in 2MP are shown in Fig. 5 for four different temperatures, from room temperature to below the 2MP glass transition temperature ($T_g = 80$ K). First consider the 298 K spectrum. The strong absorption peak near 2278 cm^{-1} has been attributed to the N=C=O antisymmetric stretching vibration, ν_{AS}.[18] Several other features at lower energy are visible in the spectrum: one located at ~2260 cm^{-1} and one at ~2220 cm^{-1}. A normal mode analysis of EIC using MACSPARTAN and a search of the literature reveals that these are not fundamental vibrational modes of the molecule; we attribute them to various combination bands of lower-frequency modes, possibly $\nu_7 + \nu_{12}$ or $\nu_{10} + \nu_{11}$, as reported by Durig *et al.*[19] These same peaks appear in the spectra at all temperatures, and are essentially temperature independent. In the 298 K spectrum, the 2260 cm^{-1} peak appears as a shoulder on the side of the main peak. In the 61 K spectrum, the 2260 cm^{-1} peak appears distinct from the shoulder at ~2274 cm^{-1}. These combination band peaks play no role in the line shape analysis that follows. (In the vibrational echo experiments, the bandwidth of the laser was narrow enough to avoid overlap with them.) However, the peak at 2260 cm^{-1} makes it necessary to compare calculated absorption curve shapes on the blue side (high-energy side) of the line and only partway down the red side of the line.

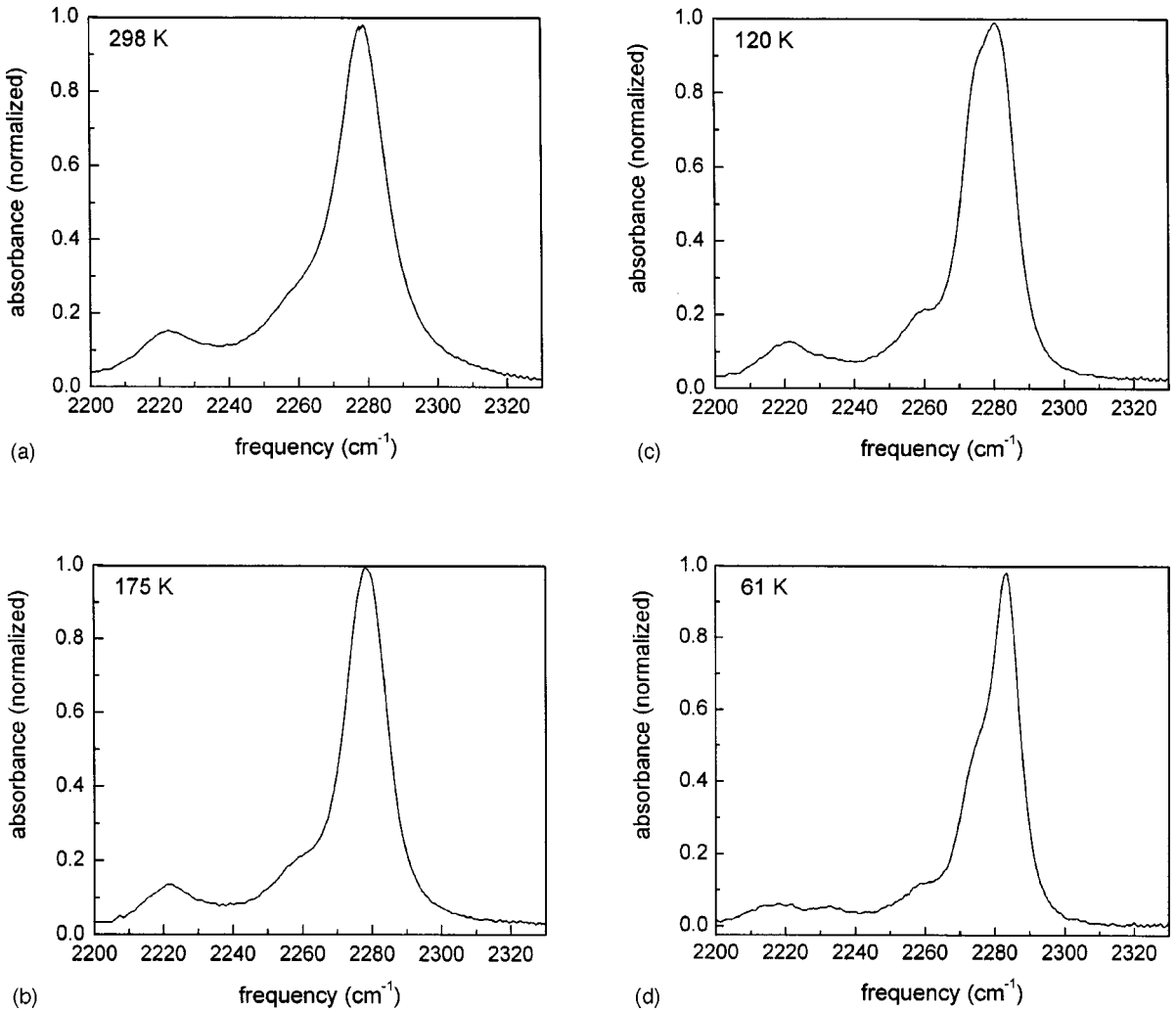

FIG. 5. Representative steady-state IR absorption spectra of the N=C=O antisymmetric stretching mode of ethyl isocyanate in 2-methylpentane with decreasing temperature: (a) room temperature (298 K), (b) 175 K, (c) 120 K, and (d) 61 K. The lines at ~2260 and 2220 cm^{-1} are combination bands that do not play a role in the analysis. By 120 K it can be seen that the main peak is separating into two lines. At 61 K, the main band is composed of two absorption lines: the *trans* conformation (2273.5 cm^{-1}) and the *gauche* conformation (2282.5 cm^{-1}). At high temperatures, a rapid exchange between the conformations has collapsed the *gauche* and trans peaks into a single band.

At room temperature (298 K) the N=C=O feature appears as a single peak at ~2278 cm^{-1}, and the line shape fits very well to a Lorentzian function. As the temperature is lowered, the N=C=O ν_{AS} feature first broadens and then splits into two spectral features: a main peak at ~2283 cm^{-1} and a shoulder near ~2274 cm^{-1}. The line becomes decidedly non-Lorentzian in shape. The onset of the separation into two lines can be seen in the 120 K spectrum near the peak; it is the very distinct shoulder in the 61 K spectrum. Below the 2MP T_g, the N=C=O ν_{AS} band stops changing as the temperature decreases, maintaining both its position and shape. In fact, all of the spectra below 86 K are so similar that they can be overlaid without a scaling factor.

The spectrum of EIC has contributions that involve direct interactions with the solvent and contributions that depend on the ethyl group. The contribution from the ethyl group can be seen clearly by comparing the EIC and the HNCO temperature-dependent spectra. The only difference between these two molecules is the replacement of the ethyl group on EIC with an H on HNCO. Figure 6 shows the HNCO in 2MP spectrum at four temperatures. The HNCO IR spectra differ drastically from those of EIC. At room temperature, the HNCO spectrum has a Lorentzian line shape, with a width almost identical to that of the room temperature EIC spectrum. Comparing the EIC and HNCO spectra only at room temperature could lead to the erroneous conclusion that the ethyl group is unimportant because it seems to make little difference at room temperature. However, unlike the spectrum of EIC, the HNCO spectrum narrows dramatically with decreasing temperature while maintaining its Lorentzian shape. By 140 K, the HNCO spectrum is ~1.5 cm^{-1} FWHM. As the temperature is lowered farther, the shape is no longer a Lorentzian. From 140 to ~110 K, the HNCO can be modeled well with the convolution of a Lorentzian with a Gaussian (i.e., a Voigt profile), making it possible to extract the Lorentzian component. Below ~110 K, the spectrum is temperature independent, presumably because it is dominated by inhomogeneous broadening. At low temperatures, below T_g, the HNCO spectrum is a single, very narrow line. In contrast, the EIC spectrum is much broader in the glass

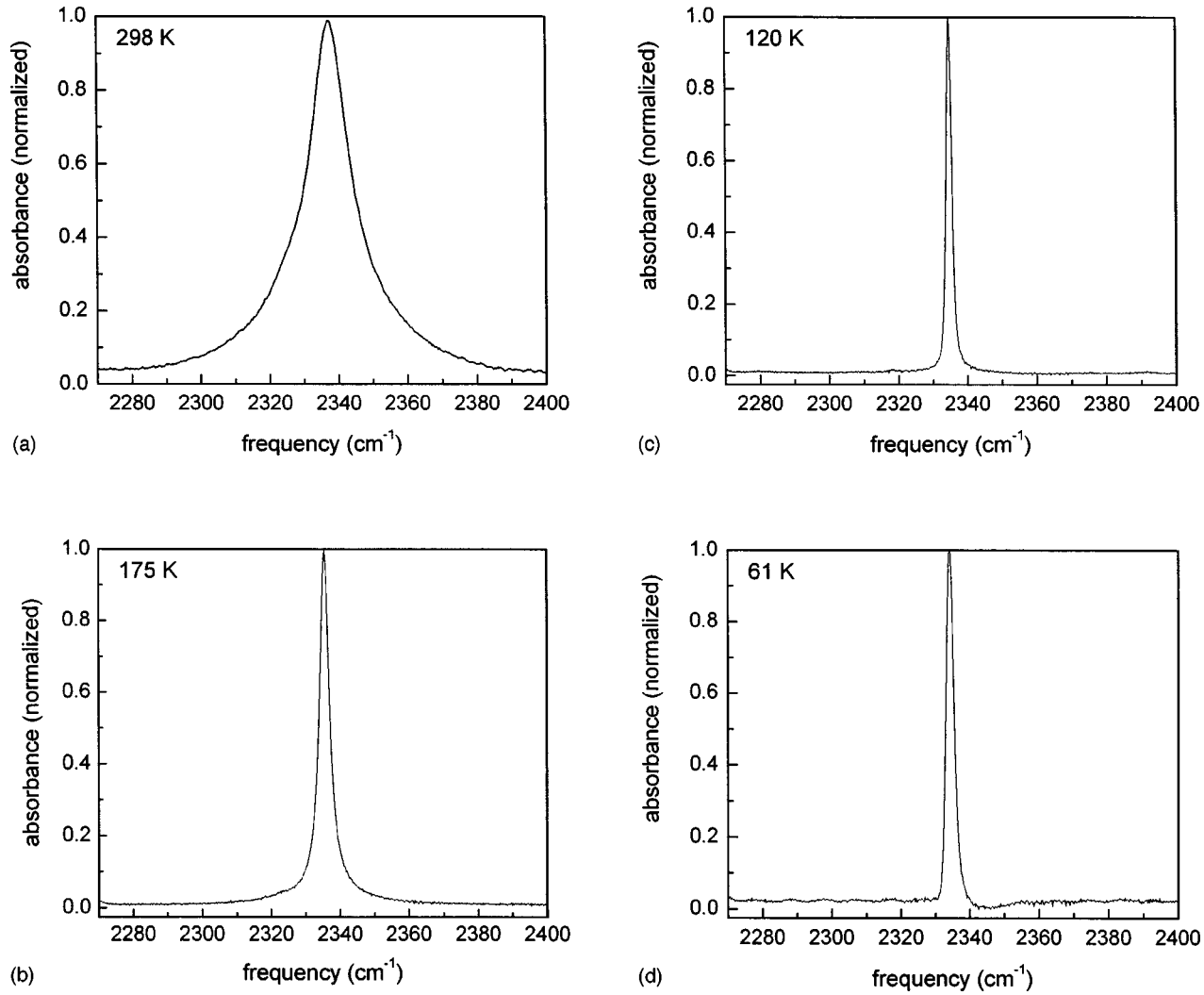

FIG. 6. Representative steady-state IR absorption spectra of the N=C=O antisymmetric stretching mode of isocyanic acid in 2-methylpentane with decreasing temperature: (a) room temperature (298 K), (b) 175 K, (c) 120 K, and (d) 61 K. At all temperatures, a single line is observed that narrows rapidly with decreasing temperature.

and is composed of two lines, as is evident by the shoulder that is clearly visible in all of the low-temperature spectra (see the 61 K spectrum in Fig. 5).

Thus, while the room temperature spectra of HNCO and EIC are very similar, their behaviors diverge significantly as the temperature is lowered. These differences demonstrate that the presence of the ethyl group in the EIC molecule greatly affects the temperature-dependent behavior of both the linewidth and line shape of the N=C=O ν_{AS} transition of EIC in 2MP.

The splitting of the N=C=O ν_{AS} peak at low temperature suggests the existence of two isomers of EIC. The orientation of the ethyl tail with respect to the N=C=O group changes the N=C=O ν_{AS} frequency, leading to two distinct spectral features observed at low temperature. Indeed, *ab initio* calculations of the vibrational spectrum of isolated EIC predict that the N=C=O ν_{AS} vibrational frequency is ~ 7 cm^{-1} higher in energy when the ethyl group is *trans* to the N=C=O moiety than when it is *gauche*.[3,4,20] While both the *trans* and *gauche* conformations are predicted to be local minima in the potential energy surface for the isolated molecule (with the gauche conformation ~ 118 cm^{-1} lower in energy than the *trans* conformation), the *cis* configuration is predicted to be a local maximum (i.e., a saddle point between the two *gauche* conformations) in the isomerization potential, and thus should not be observed.[3] The *ab initio* calculations need to be considered as qualitative input in the present context since they do not include the solvent. The solvent will contribute both enthalpy and entropy to the free energy surface. In addition, the calculation, while comprehensive, was not at a high level by today's standards. Therefore, the actual numbers obtained from the calculations cannot be utilized, but the qualitative picture of two isomers not widely separated in energy is undoubtedly correct.

IV. QUALITATIVE CONSIDERATION OF THE VIBRATIONAL ECHO AND SPECTROSCOPIC RESULTS

A. The high-temperature regime

The vibrational echo pure dephasing results (Fig. 4) display a very weak temperature dependence at high tempera-

tures with a much steeper temperature dependence at low temperatures. The EIC spectrum displays a weak but complex temperature dependence, changing from a single Lorentzian line at room temperature to two Gaussian lines at low temperature. In contrast, the HNCO spectrum is a single Lorentzian line at room temperature that narrows rapidly as the temperature is decreased, but it remains a single line.

These results suggest that the time-dependent and time-independent contributions to the EIC results can be divided into two types: intermolecular and intramolecular interactions with the N=C=O chromophore. The intermolecular interactions involve the direct interaction of the N=C=O with the solvent. The intramolecular interactions occur through the interaction of the N=C=O with the ethyl group. The direct interactions of the N=C=O with the solvent should be essentially the same for EIC and HNCO. The fact that the room temperature absorption spectra of EIC and HNCO are virtually identical indicates that direct solvent interactions dominate both the spectrum and the vibrational echo decay of EIC at room temperature.

The EIC spectrum clearly consists of two peaks at low temperature. The spectrum is separating into two peaks at intermediate temperatures (see Fig. 5, 120 K spectrum), but the spectrum is a single Lorentzian peak at room temperature. The temperature dependence of the EIC spectrum indicates that there is rapid exchange between the *trans* and *gauche* isomers at high temperatures. As in NMR, the rapid exchange between the two conformations will collapse the two peaks into a single motionally narrowed peak.[5–7] The EIC spectrum and the HNCO spectrum are almost identical at room temperature. Therefore, both spectra must be dominated by the direct intermolecular dynamic interactions with the solvent because HNCO does not have isomerization as a possible broadening mechanism. From these facts, we conclude that at room temperature, the intramolecular isomerization contribution to both the EIC vibrational echo decay and the absorption spectrum is small. The isomerization contribution will be small if the exchange time is very fast, producing a very narrow motionally narrowed ''intramolecular line.''

The very weak temperature dependence of the pure dephasing, T_2^* (see Fig. 4) above ~120 K reflects a tradeoff between the intramolecular and intermolecular temperature dependences. Assuming that the intermolecular temperature dependence is the same for the N=C=O chromophore in EIC and HNCO, the intermolecular contribution to the EIC vibrational echo decay decreases rapidly with falling temperature. However, as the temperature is lowered, the rate of isomerization will slow. As the exchange rate slows, the extent of motional narrowing will decrease, causing the line to broaden and the intramolecular contribution to the EIC vibrational echo decay to increase. The opposite temperature dependences of the intermolecular and intramolecular contributions to the dephasing produce the observed weak temperature dependence of the vibrational echo decay above ~120 K.

At the higher temperatures, the EIC vibrational echo data reflect a combination of the intramolecular and intermolecular dynamics. The intramolecular contribution can be separated from the intermolecular contribution by using the HNCO vibrational line shape data. The HNCO linewidths (Γ) were converted to dephasing times using

$$\Gamma = 1/\pi T_2 . \tag{4}$$

These dephasing times can be subtracted from the vibrational echo measured dephasing times to give the intramolecular isomerization contribution to the EIC vibrational echo data. At room temperature, the HNCO line is slightly wider than the EIC line, presumably because HNCO has a somewhat stronger coupling to the solvent. The detailed calculations presented below indicate that the intramolecular motionally narrowed isomerization contribution to the EIC is ~5% at room temperature. Therefore, we use the temperature dependence of the HNCO data but scale all of the points with a single factor so that the HNCO width is 0.95 of the EIC width at room temperature prior to subtraction.

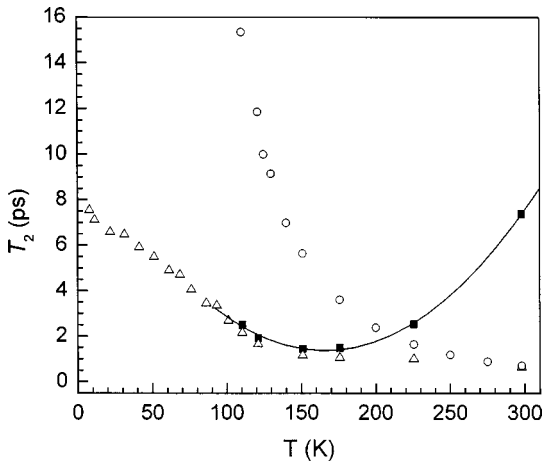

FIG. 7. A comparison of dephasing times, T_2, for the N=C=O antisymmetric stretching mode in ethyl isocyanate (△) and HNCO (○) in 2-methylpentane as a function of temperature. Using these data, the contribution to the EIC dephasing time from isomerization, T_2^i, (■) is obtained. As the temperature is first decreased, T_2^i becomes shorter because the extent of motional narrowing is reduced. The line through the squares is an aid to the eye.

The dephasing data and the results of subtraction are shown in Fig. 7. The triangles are the temperature-dependent EIC dephasing times obtained from vibrational echo measurements. The circles are the HNCO dephasing times obtained from the linewidths. The HNCO dephasing times increase rapidly with decreasing temperature mirroring the rapid narrowing of the absorption line that is evident in Fig. 6. The black squares result from subtraction of the scaled HNCO data from the EIC data. The squares are the intramolecular contribution to the EIC dephasing. The line through the squares is an aid to the eye. As shown in Fig. 7, as the temperature is decreased, the intramolecular dephasing time first becomes shorter (the line width becomes broader) before increasing at lower temperatures. The increase in the intramolecular contribution to the linewidth as T is decreased is caused by the reduction in the isomer exchange motional narrowing. The isomer exchange will rigorously produce a single line as long as $\Delta \times \tau < 1$, where Δ is the line splitting and τ is the exchange time between the two conformations.

By ~150 K, the isomerization is no longer rapid enough to collapse the two isomer absorption lines into a single line. In Fig. 5, the 175 K spectrum is a single line, while the 120 K spectrum clearly shows evidence of the two underlying *trans* and *gauche* absorption lines.

B. The low-temperature regime

As shown in Fig. 7, by ~110 K, the direct intermolecular solvent contribution to the dephasing (circles) is very small. In addition, as will be shown in detail below, the contribution from isomerization is almost negligible. By T_g (80 K), isomerization has ceased. However, the dephasing time in the low-temperature regime, as measured by the vibrational echo, is very fast compared to HNCO and other systems that have been studied.[1] Therefore, it is reasonable to assume that both the dynamics and the extent of inhomogeneous broadening in the low-temperature regime are caused by the EIC ethyl group.

To understand these data, we first, consider the inhomogeneous broadening at low temperatures. In EIC, the low-temperature band is composed of two lines: one for the *gauche* and one for the *trans* conformation (see Fig. 5, 61 K spectrum). These lines are each ~8 cm^{-1} wide. In contrast, the HNCO line in the low-temperature glass is ~1.5 cm^{-1} wide (see Fig. 6, 61 K spectrum). The HNCO width arises from the intermolecular interactions of the N=C=O chromophore with the disordered glassy solvent. Because the N=C=O chromophore of EIC will have the same intermolecular interactions with the solvent, the cause of the extensive inhomogeneous broadening must be due to small variations in the conformations of the ethyl chain. This is represented schematically in Fig. 8. The upper part of the figure shows a schematic of the isomerization potential surface.[3] At low temperatures, <110 K, in the extremely viscous liquid and in the glass, the *gauche* and *trans* surfaces are not smooth. Variations in the local solvent structure can result in variations in the configuration of the ethyl chain. These variations give rise to differences in the N=C=O transition frequency. In the low-temperature glass, the barriers between the local minima are too high to surmount. Even in the liquid near T_g, the time scale for structural evolution is so long that the N=C=O absorption line still has a significant inhomogeneous contribution.

At low temperature, each minimum of the inhomogeneous structure can itself have structure (the lowest portion of Fig. 8). However, these minima are so shallow that the system can be activated over the barriers or, with phonon assistance, tunnel through the barriers. Transitions among these shallow minima produce fluctuations in the N=C=O transition frequency and rapid low-temperature dephasing. Both the low-temperature inhomogeneous broadening and the dynamic dephasing result from the interactions of the ethyl group with the N=C=O chromophore. In contrast, HNCO has neither substantial inhomogeneous broadening nor significant dynamic dephasing at low temperatures.

Figure 8 can be used to visualize the temperature dependence of the intramolecular components of the vibrational echo data and the absorption spectrum. At the lowest temperatures, from 8 K to ~60, the transition is substantially

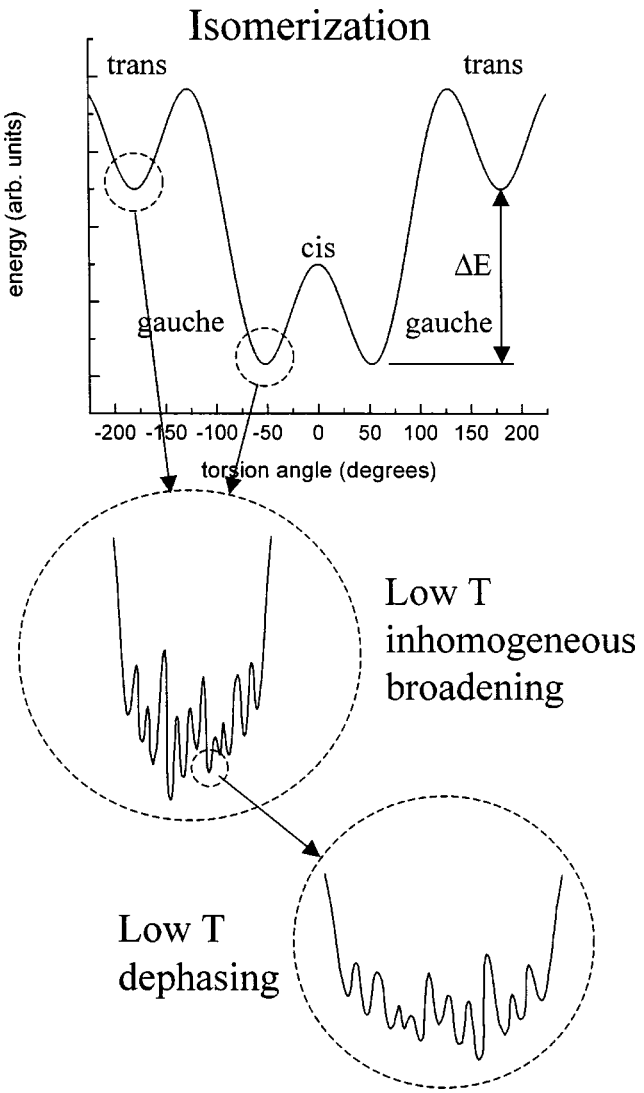

FIG. 8. Upper portion: schematic representation of the isomerization potential surface. Middle portion: expanded view of the ethyl isocyanate isomerization potential surface. Small variations in the ethyl group configuration give rise to differences in the N=C=O transition frequency. For $T \leqslant \sim 225$ K, these variations contribute to inhomogeneous broadening. Lower portion: at low temperature, each local variation (shown above) can itself have structure. Minima are so shallow that the system can be activated over the barriers or, with phonon assistance, tunnel through the barriers. Transitions among these shallow minima produce fluctuations in the N=C=O transition frequency and rapid low-temperature dephasing.

inhomogeneously broadened. The dephasing dynamics involve motions that primarily remain in the local minima that give rise to the inhomogeneous broadening (the middle part of Fig. 8). As the temperature is raised further, transitions among these local minima can occur. At higher temperatures (>~100 K), the amplitudes of the ethyl motions in the *trans* and *gauche* potential minima become sufficiently large that some isomerization can occur. Up to ~150 K, the isomerization is slow enough that there are still two distinct lines. However, the exchange between *trans* and *gauche* configurations causes significant dephasing, broadening the lines and shifting them toward each other (see Fig. 5, 120 K spectrum). In this temperature range (~100–150 K), both motion in the *trans* and *gauche* minima and isomerization contribute to the dephasing. By 175 K, the isomerization is so fast that

the two lines have undergone exchange collapse into a single line, and motions within the individual minima are no longer important. As the temperature is raised from 175 K to room temperature, the intramolecular isomerization contribution to the dephasing and absorption spectrum is reduced by motional narrowing (see Fig. 7, squares). In addition to the intramolecular contributions to dephasing and the absorption line shape, the intermolecular direct interaction with the solvent dynamics plays a significant role at higher temperatures (see Fig. 7, circles). The increase in the dephasing caused by the intermolecular dynamics at high temperature offsets the decrease in dephasing caused by motional narrowing between 175 and 298 K. The result is the very weak temperature dependence of the vibrational echo pure dephasing at the higher temperatures (see Fig. 4).

V. A MODEL FOR THE COMBINED SPECTROSCOPIC AND VIBRATIONAL ECHO DATA

In this section, the ideas presented qualitatively in Sec. IV are modeled theoretically. The model captures the essential features of the problem using a relatively simple approach. While the method shows a remarkable ability to combine the various aspects of the problem and thereby reproduce the temperature dependence of the EIC absorption spectrum, the numerical results, for example, the isomerization times at each temperature, could have some systematic error.

The time scales probed in vibrational spectroscopy are much faster than those studied in NMR. While the concept of motional narrowing exists in vibrational spectroscopy,[7,21] the short time scale for vibrational dephasing, caused in part by influences other than isomerization, makes it difficult to separate the exchange contribution to the dephasing from the direct intermolecular solvent-induced dephasing.[7,21] Contributions from solvent-induced dephasing and inhomogeneous broadening cannot be neglected. However, the basic concepts of the effect of interconversion between two spectrally distinguishable molecular configurations, such as *trans* and *gauche* isomers of EIC, still hold. Thus, we employ NMR exchange formalism in the data analysis.[5,6] The additional contributions of solvent-induced dephasing and inhomogeneous broadening are included through convolution, as discussed below.

In NMR, the spectral line shape is obtained from the imaginary portion of the expression for the magnetization.[5,6] $F(\omega)$ is the spectral line shape in the limit that the line shape is dominated by exchange between two different molecular forms, A and B:

$$F(\omega)\propto\frac{P_{\mathrm{AB}}P_{\mathrm{BA}}(\omega_{\mathrm{A}}-\omega_{\mathrm{B}})^2}{(P_{\mathrm{AB}}+P_{\mathrm{BA}})(P_{\mathrm{BA}}(\omega-\omega_{\mathrm{A}})+P_{\mathrm{AB}}(\omega-\omega_{\mathrm{B}}))^2+(\omega-\omega_{\mathrm{A}})^2(\omega-\omega_{\mathrm{B}})^2}, \tag{5}$$

where P_{AB} is the probability of making a transition from state A to state B in the time interval δt, and P_{BA} is the probability of making a transition from state B to state A in the time interval δt. ω_{A} is the frequency of A in the absence of exchange, and ω_{B} is the frequency of B in the absence of exchange. f_a and f_b are the fractions of molecules in configurations A and B, respectively, and are given by

$$f_{\mathrm{A}}=\frac{P_{\mathrm{AB}}}{P_{\mathrm{AB}}+P_{\mathrm{AB}}},\quad f_{\mathrm{B}}=\frac{P_{\mathrm{BA}}}{P_{\mathrm{AB}}+P_{\mathrm{BA}}}. \tag{6}$$

Taking state A to be lower in energy than state B, then the rate for the upward transition, P_{AB}, is the probability of the downward transition, P_{BA}, scaled by a Boltzmann factor,

$$P_{\mathrm{AB}}=P_{\mathrm{BA}}e^{-\Delta E/\kappa_{\mathrm{B}}T}. \tag{7}$$

As mentioned above, the exchange formula, Eq. (5), cannot be considered in the absence of other broadening mechanisms. Thus we combine Eq. (5) with the other aspects of the problem to calculate the temperature-dependent absorption spectrum. For temperatures at which the absorption data were measured but vibrational echo data were not measured, the vibrational echo values are obtained by interpolation between the available points. The calculation of the EIC absorption spectrum falls into three temperature regimes: high, intermediate, and low.

In the high-temperature regime, the absorption line shape is dominated by the direct intermolecular interaction with the solvent and the intramolecular isomerization. These dynamics govern the observed line shape from 298 to ~200 K. In addition, as the temperature is lowered, inhomogeneous broadening contributes to the line shape. The following procedure is used to fit the spectra in this temperature regime. All of the direct solvent-induced dephasing times obtained from the HNCO spectra are multiplied by a single constant so that at 298 K the HNCO spectroscopic width is 95% of the EIC width (see the discussion in Sec. IV A). The resulting widths, $1/\pi T_2^d$, are used as the direct solvent contributions to the EIC linewidths. Assigning a 5% contribution to the isomerization portion of the dephasing at room temperature produces the best overall agreement with the temperature dependence of the data. Varying this value by $\pm 2\%$ yields only a small difference. However, outside of this range, the temperature-dependent fits degrade substantially. The isomerization contribution to T_2, T_2^i, is obtained from

$$\frac{1}{T_2^i}=\frac{1}{T_2}-\frac{1}{T_2^d}. \tag{8}$$

The exchange line shape equation, Eq. (5), is then used to produce a calculated line at each temperature to match the value of T_2^i. At each temperature, the exchange line shape is convolved with a Gaussian, to account for inhomogeneous broadening, and subsequently convolved with a Lorentzian, $1/\pi T_2^d$, to account for the direct solvent contribution.

TABLE I. Parameters used in the fits of the linear IR spectra. τ_j—jump time, the inverse of jump rate used in the exchange calculation; ΔE—energy difference between *gauche* and *trans* lines. The gauche configuration is lower in energy; widths—the columns labeled *w* are full width half-max; w_G—width of Gaussian inhomogeneous contribution to the absorption lines; $w_{L,d}$—width of Lorentzian contribution to the absorption lines from the direct interaction with the solvent; $w_{L,m}$—width of Lorentzian contribution to the absorption lines from motions of the ethyl group that do not lead to isomerization.

Temperature (K)	τ_j (ps)	ΔE (cm^{-1})	w_G (cm^{-1})	$w_{L,d}$ (cm^{-1})	$w_{L,m}$ (cm^{-1})
298[a]	2.2	<20	⋯	14.9	⋯
275[a]	4.8	<20	⋯	11.8	⋯
250	7.4	<20	⋯	8.9	⋯
225	7.5	<20	6	6.4	⋯
200	10	15	8	4.5	⋯
175	10	15	8	2.9	1.7
150	20	15	8	1.9	1.8
140	20	15	8	1.5	1.8
130	25	15	8	1.1	2.4
125	28	20	8	1.2	2.5
120	45	20	8	0.9	3.4
115	70	20	8	0.8	3.4
110	90	20	8	0.7	3.2
101	∞	30	8	0.7	
93	∞	42	8	0.2	
86	∞	54	8	⋯	

There are three fitting parameters in this procedure: the jump time (P_{AB}) and the energy difference between the potential minima of the *trans* and *gauche* isomers in the exchange model, ΔE [see Eq. (7) and see Fig. 8], and the inhomogeneous width (w_G). The separation between the lines in the absence of exchange was determined from low-temperature spectra. The splitting is 9 cm^{-1}. This value is used at all temperatures. In the high-temperature regime, the jump time, P_{BA}, and ΔE are determined from T_2^i. w_G was adjusted to give the best fit to the spectrum at each temperature, and was found to be temperature independent below 225 K within experimental error (see Table I).

Figure 9 shows the line shape data and the calculated curves for the high-temperature regime (298–200 K). As can be seen in the figure, the agreement between the data and the calculated curves is excellent. The parameters used to fit the data in the three temperature regimes are displayed in Table I. At 298 K, the line shape is rigorously in the motional narrowing limit. The motional narrowing limit occurs when $\Delta \times \tau_j < 1$, where Δ is the separation of the two lines in the absence of exchange and τ_j is the jump time. At 298 K, $\Delta \times \tau_j = 0.59$. The system is homogeneously broadened; the inhomogeneous contribution to the line shape is zero. By 200 K, $\Delta \times \tau_j = 2.7$, and the system is moving away from the motionally narrowed regime in which the two lines are completely collapsed into a single line. However, the experimentally observed absorption line still appears to be a single line, and its shape remains basically Lorentzian. By 225 K, the extent of inhomogeneous broadening has increased to 8 cm^{-1} (see Table I). This value of the inhomogeneous broadening is essentially the same for all lower temperatures. The value of ΔE in the high-temperature regime was found to be <20 cm^{-1} (see Table I). Larger values of ΔE could not reproduce the temperature trends in the curves in the high-temperature regime. However, any value <20 cm^{-1} yields the same fit in the high-temperature regime.

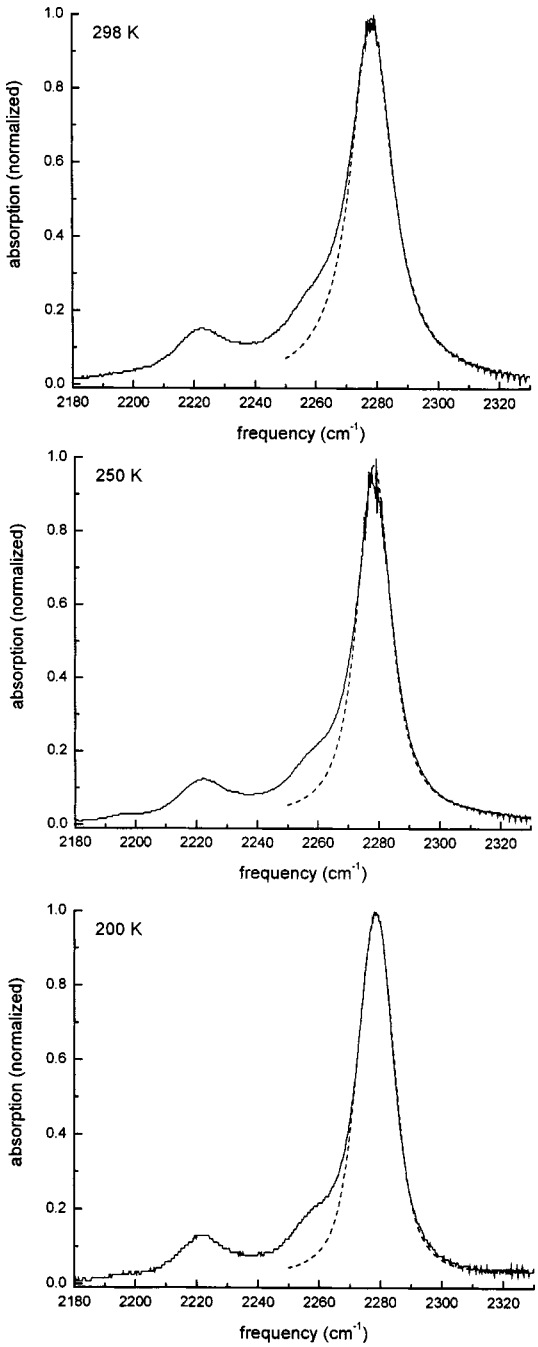

FIG. 9. Representative ethyl isocyanate antisymmetric stretch steady-state IR absorption spectra and calculated spectral line shapes in the high-temperature regime. The calculations include the effects of isomerization [Eq. (5)], direct dynamic solvent interactions obtained using the HNCO data, and inhomogeneous broadening. The agreement between the calculations and the data is excellent except on the red side, where the combination band at ~2260 cm^{-1} overlaps the antisymmetric stretch spectrum.

In the low-temperature regime ($\leqslant$101 K), the calculation of the absorption line shapes is straightforward. At low temperatures, isomerization makes a negligible contribution to the dephasing. In the glass, isomerization does not occur, but even in the very viscous liquid just above T_g, extrapolation of the jump times from higher temperatures shows that

isomerization can be neglected as a contribution to the line shape. In addition, the contribution from the direct solvent-induced dephasing is very small. For the temperatures 101 and 93 K, extrapolation of the direct contribution curve (Fig. 7, circles) is used to estimate the direct contribution. Below 93 K, it is taken to be zero. Therefore, the main contributions to the line shape are the dynamic dephasing associated with motions of the ethyl group around the bottom of the *gauche* and *trans* well that do not lead to isomerization (see the discussion in Sec. IV B and Fig. 8). The relative heights of the two lines that comprise the total line shape do not change with temperature near and below T_g. In the liquid, somewhat above T_g, the jump time is very long, but it can still bring the *gauche* and *trans* isomers into thermal equilibrium. As the temperature approaches T_g, the time scale to achieve thermal equilibrium between the two isomers becomes longer than the time spent at each temperature as the temperature is lowered. Below ~93 K, the ratio of the amplitudes of the two peaks is locked in and no longer reflects the true Boltzmann factor.

At the low temperatures, two lines separated by ~9 cm^{-1} comprise the spectra. Because the jump times between the *trans* and *gauche* configurations are very long or infinite, the exchange model can be replaced by a pair of Lorentzian line shapes, which account for the dynamic broadening processes other than isomerization. The dynamic broadening is convolved with a Gaussian to account for the inhomogeneous broadening (Voigt profile). The spectra fit well to the sum of two Voigt line shapes, as shown in Fig. 10. The Lorentzian component is determined by the vibrational echo decay, that is, $1/\pi T_2$. The widths and relative amplitudes of the two Gaussians are obtained by fitting. As at the higher temperatures, the Gaussian widths, w_G, are all 8 cm^{-1}. The parameters used to reproduce the absorption spectra are listed in Table I. Note that the ΔE value is larger at low temperature than at high temperature. This fact will be discussed in the context of the analysis of the intermediate temperature regime, which is the most complex. Between 86 and 61 K, the only change in the line shapes is a reduction in the Lorentzian contribution. The Lorentzian contribution is obtained directly from the vibrational echo measurements using the data in Fig. 2(a). At 86 K, the Lorentzian contribution is 2.9 cm^{-1}, which is small compared to the inhomogeneous width of 8 cm^{-1}. Below 61 K, the line shapes are determined solely by inhomogeneous broadening; they are identical. Between 86 and 61 K, the Lorentzian contribution is so small that its affect on the line shapes is almost negligible.

In the high-temperature regime motions of the ethyl group lead to isomerization, which contributes to the absorption line shape as $1/\pi T_2^i$. In the low-temperature regime, motions of the ethyl group do not result in isomerization and contribute to the absorption line shape as $1/\pi T_2^m$. In the intermediate-temperature regime, the absorption line shape has contributions from both types of motions. Furthermore, in the intermediate-temperature regime, isomerization does not lead to complete collapse of the two absorption lines into a single line. Isomerization [Eq. (5)] produces a complex-shaped spectrum that contributes to the overall line shape. In addition, in the intermediate-temperature region, the direct solvent dephasing is non-negligible.

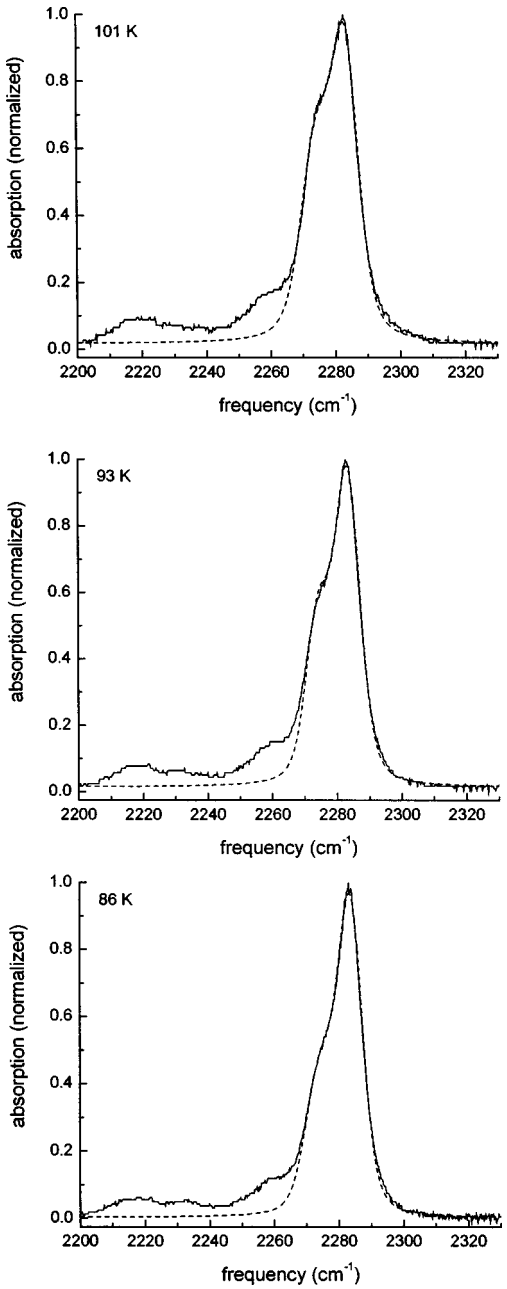

FIG. 10. Representative ethyl isocyanate antisymmetric stretch steady-state IR absorption spectra and calculated spectral line shapes in the low-temperature regime. The calculations include the effects of motions of the ethyl group that do not lead to isomerization and inhomogeneous broadening. At low temperatures, the contributions from isomerization and solvent dynamics are negligible. The agreement between the calculations and the data is excellent except on the red side, where the combination band at ~2260 cm^{-1} overlaps the antisymmetric stretch spectrum.

As can be seen in Fig. 5, the 120 K spectrum shows the beginning of the separation of the spectrum into two peaks. The isomerization contribution to the line shape determines this aspect of the line shape. All other factors contribute equally to the two lines, and do not determine the separation of the lines. Figure 11(a) illustrates the initial steps used in calculating the line shape at intermediate temperatures. Parameters are selected for the exchange calculation, that is, the

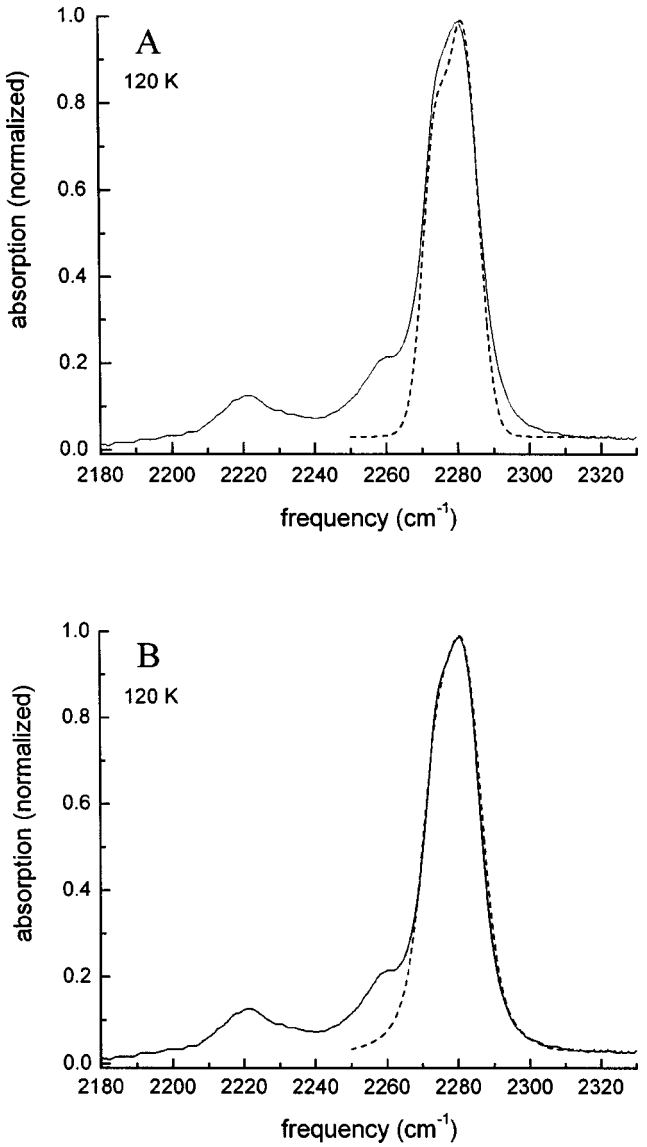

FIG. 11. Steady-state IR spectrum of the N=C=O antisymmetric stretching mode in ethyl isocyanate in 2-methyl pentane at 120 and two stages of calculation of the spectrum for the intermediate temperature regime. (a) Exchange model fit [Eq. (5); see the text] including direct solvent and inhomogeneous broadening contributions. The agreement is not good around the peak of the spectrum and in the high-energy wing. (b) The effect of the motions of the ethyl group that do not lead to isomerization is included in the calculation. The agreement between the data and the calculation is excellent except on the low-energy side, where the combination band at 2260 cm^{-1} overlaps the spectrum.

jump time and ΔE. The resulting exchange line shape is convolved with the Lorentzian direct contribution (Fig. 7—circles; Table I—$w_{\mathrm{L},d}$) and then convolved with the inhomogeneous Gaussian profile. While, the inhomogeneous width is treated as an adjustable parameter, the result is always 8 cm^{-1}. The parameters in the exchange calculation are varied until the region around the peak of the spectrum is fit as well as possible. As can be seen in Fig. 11(a), this procedure is able to produce a rough approximation of the spectrum. However, it misses around the peak, and it does not reproduce the broad wings of the line, as can be seen in the wavelength range from 2290 to 2310 cm^{-1}. The low-energy wing of the line is obscured by combination bands (see Sec. III B).

The calculation of the spectrum in Fig. 11(a) does not fit the data well because the ethyl group motions other than isomerization have not been included. The total dynamic dephasing is measured by the vibrational echo decay. The vibrational echo data can be used to determine the additional contribution, $1/\pi T_2^m$, to the absorption line shape. In the intermediate temperature range, for example 120 K, the exchange contribution to the spectrum can be reasonably approximated as the sum of two displaced Lorentzians. The Lorentzian linewidth, $1/\pi T_2^i$, is used to determine T_2^i. The direct solvent contribution, T_2^d, is also known (Table I—$w_{\mathrm{L},d}$). Then T_2^m is determined from the vibrational echo data using

$$\frac{1}{T_2^m}=\frac{1}{T_2}-\frac{1}{T_2^i}-\frac{1}{T_2^d}. \tag{9}$$

Therefore, T_2^m is not an independent adjustable parameter. The T_2^m contribution to the line shape is included by convolving a Lorentzian with width $1/\pi T_2^m$ with the line shape as in Fig. 11(a). The values of $w_{\mathrm{L},d}$ (full width at half-max of the Lorentzian direct solvent contribution) used for the intermediate temperature calculations are listed in Table I. The procedure yields very good agreement with the data, but the agreement can be improved by then making a small adjustment in T_2^i, recalculating T_2^m, and then calculating the final line shape. The result of this procedure is shown in Fig. 11(b) for the 120 K spectrum. The calculated spectrum now agrees with the measured spectrum exceedingly well. The calculated spectrum in Fig. 11(b) fits the region around the peak of the spectrum and in the wings of the spectrum.

While the procedure is approximate, it is clear that it is adequate to give a very reasonable description of the absorption line shape. The overall method, combining the vibrational echo decay data with the linear absorption spectra of EIC and HNCO permits the EIC spectrum to be separated into a direct solvent contribution, an isomerization contribution, an ethyl group motion (no isomerization) contribution, and an inhomogeneous contribution. Figure 12 shows the results of this fitting procedure for several of the spectra taken at intermediate temperatures. The figure shows that the agreement between the absorption spectrum data and the calculations is nearly perfect. In these computations, only parameters associated with the exchange part of the calculation are adjustable, and these are very tightly constrained by the shape of the spectrum around its maximum.

One aspect of the parameters in Table I that may be unexpected is that the value of ΔE changes with temperature. In the high-temperature regime, only a limit on ΔE could be determined. However, at intermediate temperature and low temperature, once two peaks can be discerned, the shape of the calculated spectrum is quite sensitive to ΔE. From room temperature through 130 K, a value of $\Delta E = 15\,\mathrm{cm}^{-1}$ works consistently. From 125–110 K, the value has increased to 20 cm^{-1}. Below 110 K, ΔE increases significantly until it is locked in at 86 K. This could be an artifact of the approximate approach used in the calculations.

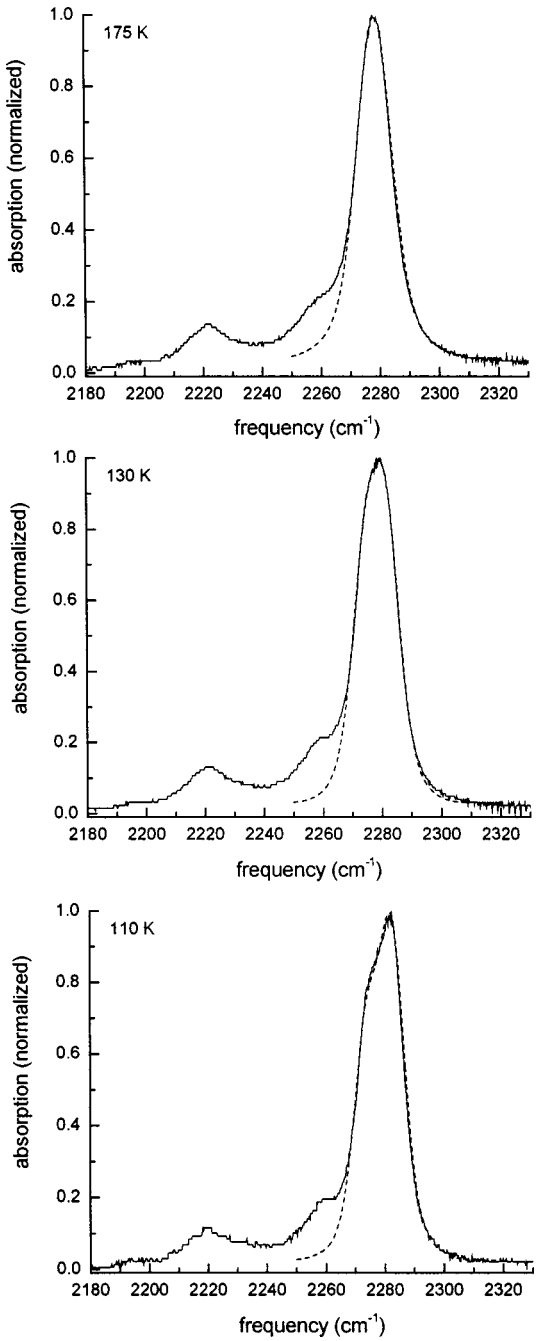

FIG. 12. Representative ethyl isocyanate antisymmetric stretch steady-state IR absorption spectra and calculated spectral line shapes in the intermediate temperature regime. The calculations include the effects of isomerization [Eq. (5)], motions of the ethyl group that do not lead to isomerization, direct dynamic solvent interactions, and inhomogeneous broadening. The agreement between the calculations and the data is excellent except on the red side, where the combination band at $\sim$2260 cm^{-1} overlaps the antisymmetric stretch spectrum.

Another explanation is that the potential surface depends on both intramolecular and intermolecular coordinates. As the temperature is lowered, the properties of the solvent change, for example, the density of the solvent increases. Therefore, it is possible that the difference in energy of the *gauche* and *trans* configurations is actually temperature dependent.

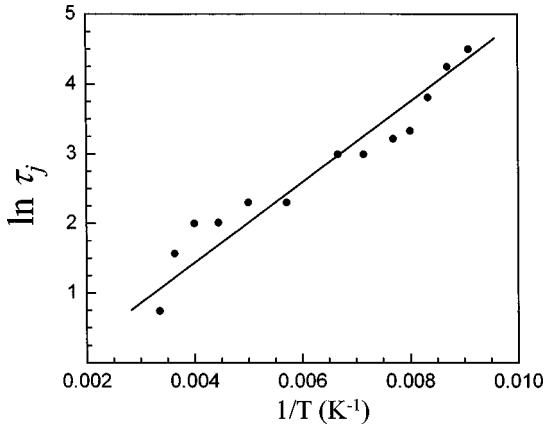

FIG. 13. An Arrhenius plot of the isomerization times, τ_j (inverse of the isomerization rate). While there is significant scatter in the points, they are reasonably well represented by a line over four factors of *e*. The slope yields the *gauche–trans* isomerization barrier of 400 ± 50 cm^{-1}.

VI. ISOMERIZATION RATES AND THE ISOMERIZATION BARRIER HEIGHT

The analysis presented above explains the nature of the temperature-dependent dynamics, the absorption line shapes, and the vibrational echo data. One of the main features of the experiment is its observation of very fast isomerization occuring on the ground state potential surface. The EIC *gauche–trans* isomerization is not laser induced as in, for example, the *cis–trans* stilbene isomerization, which occurs following electronic excitation.[22,23] As has been pointed out, it is difficult to obtain thermal isomerization rates from the analysis of temperature-dependent vibrational spectra alone because of the other contributions, dynamic and static, to the line shape.[7,21] By combining vibrational echo experiments with linear spectroscopic measurements, we have been able to separate the various contributions to the vibrational dephasing and line shapes. The results yield the temperature-dependent *gauche–trans* isomerization times, τ_j, (inverse of the isomerization rates) listed in Table I.

Figure 13 shows an Arrhenius plot of the τ_j, that is, a plot of $\ln(\tau_j)$ versus $1/T$. While there is considerable scatter, the plot shows that the points can be reasonably taken to fall on a line. The line through the points yields an estimate of the activation energy (barrier height) for the isomerization of 400 ± 50 cm^{-1}. The isomerization occurs when the EIC methylene rotates around the nitrogen–methylene carbon bond. The simplest picture of the bonding in EIC would assign an sp^2 hybrid to the N, with the N=C=O linear and the methylene carbon, making a 120° angle with the linear N=C=O. Quantum chemistry calculations show that the N=C=O is almost linear, but the methylene carbon–N=C=O angle is 138°.[3] In ethane, the rotation of a methyl group around the C–C bond is hindered by the steric interaction of the three hydrogens on one methyl with the three hydrogens on the other methyl. The barrier to rotation is 1030 cm^{-1}.[24]

The rotation of EIC methylene around the N–C bond should have less steric hindrance than that of ethane. Examples of molecules with less steric hindrance are acetaldehyde and methanol, which have a barrier to rotation of 425 and 390 cm^{-1}, respectively.[24] These qualitative consider-

ations suggest that the value of the barrier height obtained for the EIC *gauche–trans* isomerization is reasonable.

VII. CONCLUDING REMARKS

The temperature-dependent dynamics of the antisymmetric stretching mode of ethyl isocyanate are complex. At high temperatures, *gauche–trans* isomerization is very rapid ($\sim$2 ps) and direct dynamical interactions of the solvent with the isocyanate are substantial. The isomerization is so fast that the individual *gauche* and *trans* absorption lines are motionally narrowed into a single line. As the temperature is reduced, the rate of isomerization and the extent of the direct solvent interactions decrease. However, these two processes have opposite effects on the dynamic dephasing and the line shape. The reduced rate of isomerization takes the system away from the motionally narrowed limit. At sufficiently low temperature, the absorption spectrum changes from a single peak into two peaks. The contributions from isomerization and direct dynamical solvent interactions become negligible, but the dynamic dephasing, measured with the vibrational echoes, is still fast because of motions of the ethyl group that do not result in isomerization.

The theoretical method used to combine the various experimental observables into calculations of the temperature-dependent vibrational line shapes (Figs. 9–12) does an excellent job. However, this method is approximate. It separates the contributions to the line shape into parts. The contribution from isomerization was included using a NMR-type exchange calculation. The other contributions, direct solvent interactions, motions of the ethyl group that do not produce isomerization, and inhomogeneous broadening, were included through convolutions. While the agreement with the data is excellent, there is the question of whether a theoretical method that did not treat each aspect as independent would produce different results, particular the temperature-dependent isomerization rates. The theoretical problem is extremely difficult and unsolved. It involves calculating the influence on dephasing of isomerization when the transition energies are fluctuating because of direct solvent dynamical interactions and motions of the ethyl group that do not result in isomerization. Here we treated the isomerization as jumping between two time-independent states. A more detailed approach would recognize that the *gauche* and *trans* states are each time evolving and that the isomerization occurs between these time-evolving states.

From the temperature-dependent isomerization rates, the barrier for *gauche–trans* isomerization was obtained. The experiments yield a barrier height of 400 ± 50 cm^{-1}. It is a challenging theoretical problem to calculate this barrier height for ethyl isocyanate in the presence of the solvent 2-methylpentane.

Finally, the information obtained on the *gauche–trans* isomerization dynamics of ethyl isocyanate could not be attained from absorption spectroscopy alone. It is necessary to take the contributions to the line shape apart to understand how the various aspects coalesce to produce the temperature-dependent absorption spectra. The analysis was made possible by combining linear absorption spectroscopy with ultrafast infrared vibrational echo and pump–probe experiments.

ACKNOWLEDGMENTS

The authors are grateful to Professor T. J. Wandless and Professor J. Brauman for many helpful conversations. This work was supported by the National Science Foundation (DMR-0088942) and the National Institutes of Health (1RO1-GM61137). N.E.L. gratefully acknowledges support for a sabbatical leave from the NSF POWRE program (CHE-0074913).

[1] K. D. Rector and M. D. Fayer, J. Chem. Phys. **108**, 1794 (1998).
[2] A. Tokmakoff and M. D. Fayer, J. Chem. Phys. **103**, 2810 (1995).
[3] M. Feher, T. Pasinszki, and T. Veszpremi, J. Am. Chem. Soc. **115**, 1500 (1993).
[4] J. F. Sullivan, D. T. Durig, and J. R. Durig, J. Phys. Chem. **91**, 1770 (1987).
[5] R. Kubo, in *Fluctuation, Relaxation and Resonance in Magnetic Systems*, edited by D. Ter Haar (Oliver and Boyd, London, 1961).
[6] A. Carrington and A. D. McLachlan, *Introduction to Magnetic Resonance* (Harper and Row, New York, 1967).
[7] K. A. Wood and H. L. Strauss, J. Phys. Chem. **94**, 5677 (1990).
[8] R. A. Ashby and R. L. Werner, J. Mol. Spectrosc. **18**, 184 (1965).
[9] T. J. Wandless (private communication, 2001).
[10] N. E. Levinger, P. H. Davis, and M. D. Fayer, J. Chem. Phys. **115**, 9352 (2001).
[11] J.-P. Zhou (private communication, 1998).
[12] S. Mukamel, *Principles of Nonlinear Optical Spectroscopy* (Oxford University Press, New York, 1995).
[13] T. C. Farrar and D. E. Becker, *Pulse and Fourier Transform NMR* (Academic, New York, 1971).
[14] P. W. Atkins, *Physical Chemistry*, 4th ed. (Freeman & Company, New York, 1990).
[15] A. Tokmakoff, A. S. Kwok, R. S. Urdahl, R. S. Francis, and M. D. Fayer, Chem. Phys. Lett. **234**, 289 (1995).
[16] K. D. Rector, A. S. Kwok, C. Ferrante, A. Tokmakoff, C. W. Rella, and M. D. Fayer, J. Chem. Phys. **106**, 10027 (1997).
[17] K. A. Merchant, D. E. Thompson, and M. D. Fayer, Phys. Rev. A **65**, 023817 (2002).
[18] J. F. Sullivan, D. T. Durig, J. R. Durig, and S. Cradock, J. Phys. Chem. **91**, 1770 (1987).
[19] J. R. Durig, K. J. Kanes, and J. F. Sullivan, J. Mol. Struct. **99**, 61 (1983).
[20] S. Cradock, J. R. Durig, and J. F. Sullivan, J. Mol. Struct. **131**, 121 (1985).
[21] K. A. Wood and H. L. Strauss, Ber. Bunsenges. Phys. Chem. **93**, 615 (1989).
[22] S. K. Kim, S. H. Courtney, and G. R. Fleming, Chem. Phys. Lett. **159**, 543 (1989).
[23] D. C. Todd, J. M. Jean, S. J. Rosenthal, A. J. Ruggiero, D. Yang, and G. R. Fleming, J. Chem. Phys. **93**, 8658 (1990).
[24] I. N. Levine, *Physical Chemistry*, 5th ed. (McGraw-Hill, New York, 2002).